NeuroImage 197 (2019) 156–166

Contents lists available at ScienceDirect

NeuroImage

journal homepage: www.elsevier.com/locate/neuroimage

Brain networks underlying tactile softness perception: A functional magnetic resonance imaging study

Ryo Kitada [a,*], Ryuichi Doizaki [b], Jinhwan Kwon [c], Tsubasa Tanigawa [d,e], Eri Nakagawa [d], Takanori Kochiyama [f], Hiroyuki Kajimoto [b], Maki Sakamoto [b], Norihiro Sadato [d,e]

[a] Division of Psychology, School of Social Sciences, Nanyang Technological University, 48 Nanyang Avenue, 639818, Singapore
[b] Department of Informatics, Graduate School of Informatics and Engineering, The University of Electro-Communications, 1-5-1 Chofugaoka, Chofu, Tokyo, 182-8585, Japan
[c] Kyoto University of Education, Fukakusa-Fujimori-cho 1, Fushimi-ku, Kyoto, 612-8522, Japan
[d] National Institute for Physiological Sciences, Nishigonaka 38, Myodaiji-cho, Okazaki, 444-8585, Japan
[e] The Graduate University for Advanced Studies (SOKENDAI), Shonan Village, Hayama, Kanagawa, 240-0193, Japan
[f] ATR-Promotions, Brain Activity Imaging Center, 2-2-2 Hikaridai Seika-cho, Sorakugun, Kyoto, 619-0288, Japan

ARTICLE INFO

Keywords:
Texture perception
Parietal operculum
Primary somatosensory cortex
Softness
Compliance
fMRI

ABSTRACT

Humans are adept at perceiving physical properties of an object through touch. Tangible object properties can be categorized into two types: macro-spatial properties, including shape and orientation; and material properties, such as roughness, softness, and temperature. Previous neuroimaging studies have shown that roughness and temperature are extracted at nodes of a network, such as that involving the parietal operculum and insula, which is different from the network engaged in processing macro-spatial properties. However, it is unclear whether other perceptual dimensions pertaining to material properties engage the same regions. Here, we conducted a functional magnetic resonance imaging study to test whether the parietal operculum and insula were involved in extracting tactually-perceived softness magnitude. Fifty-six healthy right-handed participants estimated perceived softness magnitude using their right middle finger. We presented three stimuli that had the same shape but different compliances. The force applied to the finger was manipulated at two levels. Classical mass-univariate analysis showed that activity in the parietal operculum, insula, and medial prefrontal cortex was positively associated with perceived softness magnitude, regardless of the applied force. Softness-related activity was stronger in the ventral striatum in the high-force condition than in the low-force condition. The multivariate voxel pattern analysis showed higher accuracy than chance levels and control regions in the parietal operculum/insula, postcentral gyrus, posterior parietal lobule, and middle occipital gyrus. These results indicate that a distributed set of the brain regions, including the parietal operculum and insula, is involved in representing perceived softness.

1. Introduction

One of the objectives in neuroscience is to understand how sensory information is processed in the brain. It is widely assumed that the sensory input is initially processed in a parallel-distributed manner, and then, such separately processed information is integrated to provide a unified percept (Zeki, 1998). In vision, it has been found that multiple pathways exist for processing different properties such as color, depth, and motion. On the other hand, less evidence is available on the neural mechanisms underlying tactile object processing (Kitada, 2016).

Humans are adept at perceiving object properties using touch, even when vision is unavailable. Tangible object properties are organized into two major categories: macro-spatial and material properties (Jones and Lederman, 2006). The former category, which includes the perception of shape, orientation, and location, needs some form of a spatial reference system (spatial coding) (Lederman and Klatzky, 1997). On the other hand, the latter category, which includes roughness, softness, and temperature, is expressed as intensity (intensity coding) (Lederman and Klatzky, 1997). Previous studies using multidimensional scaling have demonstrated that surface roughness and softness are highly prominent perceptual dimensions of surface textures (Hollins et al., 1993, 2000). The perceived magnitude of surface roughness is associated with inter-element spacing (e.g., distance between bumps) on the surface of an object (Lederman and Taylor, 1972), whereas the magnitude of

* Corresponding author.
E-mail address: ryokitada@ntu.edu.sg (R. Kitada).

https://doi.org/10.1016/j.neuroimage.2019.04.044
Received 25 January 2019; Received in revised form 18 March 2019; Accepted 16 April 2019
Available online 25 April 2019

perceived softness is related to object compliance, that is, the magnitude of deformation of an object under an applied force (Srinivasan and LaMotte, 1996).

Previous neuroimaging studies have demonstrated a distributed set of the brain regions involved in tactile processing of object properties (Roland et al., 1998; Stilla and Sathian, 2008; Sathian et al., 2011). In these studies, compared with tactile perception of macro-spatial properties, tactile perception of material properties revealed distinct patterns of brain activation (Roland et al., 1998; Stilla and Sathian, 2008; Sathian et al., 2011). More specifically, activity in the parietal operculum (including the secondary somatosensory cortex), insula, and occipital cortex is greater for texture perception than for perception of shape (Stilla and Sathian, 2008) and of dot location on a cardboard (Sathian et al., 2011). Neuroimaging studies focusing on one perceptual dimension of material properties have shown that activity in the parietal operculum and insula is related to the magnitude of perceived roughness (Kitada et al., 2005; Eck et al., 2016) and temperature (Craig et al., 2000). A more recent study demonstrated that the activity in a part of the occipital cortex is related to perceived roughness magnitude (Eck et al., 2013). These findings raise the possibility that compared with the macro-spatial properties, the parietal operculum, the insula, and a part of the occipital cortex are involved in extracting intensity information of material properties. If this is the case, we can expect the same brain regions to also be involved in the tactile processing of other perceptual dimensions of material properties. However, compared with the perception of roughness and temperature, the neural correlates underlying the perception of object compliance and softness have been scarcely investigated.

To the best of our knowledge, only two neuroimaging studies have examined the neural substrates of tactile perception of compliance (Servos et al., 2001; Bodegard et al., 2003). Servos et al. (2001) found that haptic identification of hardness activates the postcentral gyrus (corresponding to the primary somatosensory cortex) to a greater extent than finger movement without touching an object. However, it is not clear whether activation in this region is related to tactile input in general or specific to object hardness. Bodegard et al. (2003) examined brain activation during the haptic discrimination of spring strength, and found stronger activation in regions such as the postcentral gyrus and cerebellum than rest condition. However, as such activation can be due to tactile stimulation input, the brain networks that are involved in extracting information on compliance or softness perception are still unknown.

In the present study, we conducted a functional magnetic resonance imaging (fMRI) study to test whether the parietal operculum, insula, and occipital cortex are involved in processing magnitudes of softness. The participants estimated magnitude of objects' softness when they were pushed onto their middle fingers by a stimulator. We conducted two experiments. We examined brain regions of which activity is correlated with softness in the first experiment (localizer experiment). The softer the object becomes, the force that was imposed on the finger becomes lower. Thus, if the applied force is not manipulated, the participants may simply classify objects based on the applied force, but not softness. Thus, the possibility remains that the softness-related activity in a brain region actually reflects the magnitude of the force applied to the finger. Therefore, we examined the effect of applied force on the activity related to perceived softness in the second experiment (main experiment). We predicted that the parietal operculum, insula, and a part of the occipital cortex show activity associated with perceived softness of samples, regardless of the applied force.

2. Materials and methods

2.1. Participants

Fifty-six Japanese individuals (31 men, 25 women) aged 18–41 years (mean ± standard deviation = 23.5 ± 5.5 years) participated in the study. The localizer experiment involved 32 participants (17 men), and the main experiment involved 35 participants (19 men). Eleven volunteers participated in both experiments ($32 + 35 - 11 = 56$ participants in total). All participants were right-handed, as assessed using the Edinburgh Handiness Inventory (Oldfield, 1971). None of the participants reported prior loss of tactile sensation or a history of major medical or neurological illnesses, such as epilepsy, significant head trauma, or a lifetime history of alcohol dependence. The study was conducted in accordance with the Declaration of Helsinki. All participants provided written informed consent prior to participation. The study protocol was approved by the local medical ethics committees at the National Institute for Physiological Sciences. All procedures were performed in accordance with the approved guidelines.

2.2. Experimental design and statistical analysis

We adopted within-subject experimental designs in both experiments. The localizer experiment involved four levels of object compliance, whereas the main experiment involved three levels of object compliance and two levels of applied force. All behavioral data were analyzed using SPSS software (version 23; IBM Corporation, Armonk, NY). Bonferroni correction was applied to control for multiple comparisons. All fMRI data were analyzed using the Statistical Parametric Mapping 12 (SPM12) software package (Friston et al., 2007) (RRID: SCR_007037) in MATLAB (2017b; MathWorks, Natick, MA, USA). In the mass-univariate analysis, the statistical threshold for the spatial extent test on the clusters was set at $p < 0.05$, family-wise error (FWE) corrected for multiple comparisons. The height (cluster-forming) threshold was set at $p < 0.001$ (uncorrected). This threshold is sufficiently high to use the random-field theory to control FWE rate (Flandin and Friston, 2019). We used CoSMoMVPA toolbox to perform multi-variate voxel pattern analysis (Oosterhof et al., 2016) (RRID: SCR_014519).

2.3. Stimulus presentation

As stimuli, we used 9 spherical segments that were made of urethane elastomer covered by plastic membrane and 1 spherical segment made of fiberglass-reinforced plastic (Bioskin; Beaulax Co., Ltd., Tokyo, Japan). All of them had the same size (5-cm diameter base × 1.3-cm height). We measured the compliance of the 9 stimuli using a force tester (KES-G5; Kato Tech Co., Ltd., Kyoto, Japan) (Supplementary Fig. 1). As in the previous studies (Srinivasan and LaMotte, 1995), we defined mean vertical deformation relative to force (mm/N) as compliance. These values were logarithmically transformed because the transformed values tend to be linearly related to perceived magnitudes (Kitada et al., 2012). Subsequently, four stimuli for the localizer experiment and 3 for the main experiment were selected based on the transformed compliance values. Since thermal conductivity is different between urethane elastomer and fiberglass, and may become a confounding factor, fiberglass reinforced plastics was only used in the localizer task.

We developed an MRI-compatible stimulus presentation device. This device had two parts: a wooden frame supporting the participant's right hand, and pneumatic cylinders that push the stimuli upward onto the right middle finger. The participants wore a glove that had a hole at the tip of the right middle finger. The backside of the glove was fastened to a Velcro strip that was attached to the ceiling of the wooden frame. Two identical vitreous cylinders (30 ml) that were connected through air tube were placed inside and outside the MRI scanner. A wooden plate with the stimulus was placed on the top of the cylinder inside the MRI scanner. At the onset of each trial, the device automatically placed a weight on the top of the cylinder outside the MRI scanner, moving up the cylinder inside the scanner toward the participant's middle finger. The duration of each stimulation was approximately 2.2 s, repeated twice (4.4 s). One experimenter stood beside the scanner and wore MRI-compatible headphones (Kiyohara Optics, Tokyo, Japan).

In order to stimulate the finger with two different forces, we changed

the height of the wooden plate (where the stimulus was placed) by 5 mm. Similar to a previous study (Rajaei et al., 2018), we measured the force applied to the finger by placing an air pressure sensor ($3.5 \times 3.5\ cm^2$) (Minamoto Medical, Chiba, Japan) where the participant's right finger was placed. This measurement was conducted with the same apparatus outside of the scanner. The pressure sensor was connected to a data acquisition device (ML846 PowerLab 4/26; ADInstruments, Dunedin, NZ) through a custom-made force measurement interface (Minamoto Medical). Standard Windows-based software (LabChart, ADInstruments) was used to record the force. As Fig. 1B shows, the force applied to the sensor decreases as the compliance of the stimulus increases because softer stimuli cause more deformation when they are pushed onto the sensor. Nevertheless, the force detected by the sensor was clearly different between high-force and low-force experiments (Fig. 1B). The experimenters (R.K., R.D., J.K., and T.T.) confirmed that they could clearly perceive the difference in the applied force.

Participants lay in the supine position. Participants' heads were fixed using foam pads and tape to minimize movement, and they were instructed to remain relaxed during scanning. The participants were asked to extend their arms, placing their right hand in the wooden frame. They held a response box in their left hand. Visual stimuli were presented to the participants using the Presentation software (Neurobehavioral Systems, Inc., Albany, CA, USA) implemented on a personal computer (dc7900; Hewlett-Packard, Ltd., Palo Alto, CA, USA). A liquid crystal display projector (CP-SX12000; Hitachi, Ltd., Chiyoda, Tokyo, Japan) located outside and behind the scanner projected the stimuli through a waveguide to a translucent screen, which the participants viewed via a mirror placed in the MRI scanner. The same software was used to present auditory cues for the next stimulus to be presented and the timing of replacing the stimulus with the next one. The auditory cues were only presented to the experimenter via headphones.

2.4. Data acquisition

The present study utilized a 3-T whole-body MRI scanner (Verio; Siemens, Erlangen, Germany) with a 32-element phased-array head coil. To obtain T2*-weighted (functional) images, we employed a multiband echo-planar imaging (EPI) sequence that collected multiple slices simultaneously, reducing the repetition time (TR) per volume (Feinberg et al., 2010). Specifically, the following parameters were used to cover the whole brain: gradient-echo EPI, TR = 1000 ms, multiband factor = 6, echo time (TE) = 35 ms, flip angle = 65°, 60 axial slices of 2-mm thickness with a 25% slice gap, field-of-view = $192 \times 192\ mm^2$, and in-plane resolution = $2.0 \times 2.0\ mm^2$. Further, T1-weighted high-resolution anatomical images were acquired for each participant using magnetization-prepared rapid acquisition gradient echo (MP-RAGE)

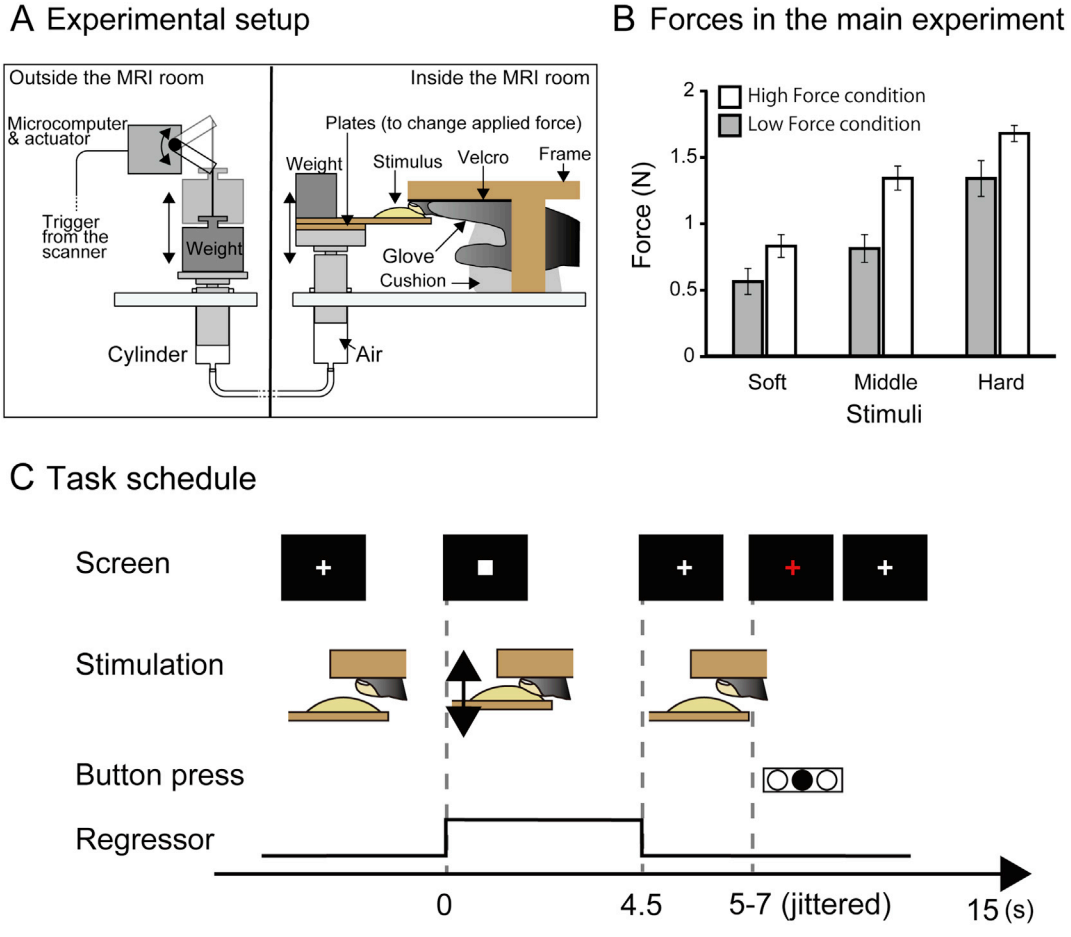

Fig. 1. Experimental design.
(A) Setup. We developed an apparatus consisting of two cylinders that are connected via an air tube. A weight was placed on the cylinder outside the scanner, which moved the stimulus onto the participant's middle finger placed inside the scanner. The stimuli had identical shapes and sizes, whereas their compliances, deformation per applied force, were varied (see Supplementary Fig. 1 for details). **(B) Forces applied to the finger.** We applied two different levels of force to the finger in the main experiment, since the force applied decreases with higher compliance. Forces were measured by placing a sensor where the finger is placed. The bar graph indicates force averaged over six trials (with SEM). **(C) Task schedule.** In each trial, the fixation cross was replaced with a white square and the stimulus was pushed onto the finger twice during the next 4.4 s. The participant was asked to judge compliance of the stimulus by pressing a button when the red fixation cross was presented. The timing of presentation of the red fixation cross was jittered.

sequences (TR = 1800 ms, TE = 1.98 ms, flip angle = 9°, and voxel size = 1 × 1 × 1 mm^3).

2.5. Task (main experiment)

Each participant completed 6 runs of the task, which included each of the 7 conditions: high compliance with the higher force (Soft-high F), high-compliance with the lower force (Soft-low F), medium compliance with the higher force (Med-high F), medium compliance with the lower force (Med-low F), low compliance with the higher force (Hard-high F), low compliance with the lower force (Hard-low F), and no stimulation condition (Baseline).

A single run consisted of twenty-one 15-s trials (315 s in total) preceded by 20-s rest and followed by 10-s rest (315 + 20 + 10 = 345 s in total, 345 vol). Each condition was repeated 3 times in a single run (3 repetitions × 6 runs = 18 trials for each condition). The order of the 7 conditions in each run was pseudo-randomized. In each trial, a white cross was replaced with a white box for 4.5 s (Fig. 1C). During this period, the participant's middle finger was stimulated in all tactile-stimulation conditions, whereas no stimulation was provided in the Baseline condition. After this period, the red cross was presented for 2 s, during which the participant pressed one of the three buttons with their left hand to indicate how soft the object felt. The order of the button presses was counterbalanced across the participants to avoid any association between response buttons and object compliance. The onset of the red cross was jittered within 2 s (5–7 s from the onset of the trial). The response was calculated as perceived softness magnitude, by treating soft as 3, middle as 2, and hard as 1. During the rest of the trial, the participant was asked to stay still and the experimenter replaced the stimuli and plates.

2.5.1. Data processing and analysis

The first 15 vol of each fMRI run were discarded to allow the MR signal to reach a state of equilibrium. The remaining volumes were used for the subsequent analyses. To correct for head motion, functional images from each run were realigned to the first image and again realigned to the mean image after the first realignment. The T1-weighted anatomical image was co-registered to the mean of all realigned images. Prior to co-registration, the T1-weighted anatomical image was skull-stripped to prevent non-brain tissue from affecting the alignment between the EPI and T1 images. Each co-registered T1-weighted anatomical image was normalized to the Montreal Neurological Institute (MNI) space using the DARTEL procedure (Ashburner, 2007). More specifically, each anatomical image was segmented into tissue class images using a unified segmentation approach. Gray and white matter images were registered and normalized to space using the preexisting template that is based on the data from 512 Japanese individuals scanned at the National Institute for Physiological Sciences. The parameters from DARTEL registration and normalization were then applied to each functional and T1-weighted anatomical image. The normalized functional images were filtered using a Gaussian kernel of 4-mm full-width at half-maximum (FWHM) in the *x*, *y*, and *z* axes. We then conducted mass-univariate analysis and multi-voxel pattern analysis (MVPA), as explained below.

2.5.2. Mass-univariate analysis

A general linear model was fitted to the fMRI data for each participant. The blood-oxygen-level dependent (BOLD) signal for the period of tactile stimulation was modelled using boxcar functions convolved with the canonical hemodynamic response function. We conducted the following two analyses, where a design matrix comprising the 6 runs was prepared for each participant.

2.5.2.1. First analysis (analysis of variance). In the first analysis, we evaluated brain activity showing main effects of each factor and the interaction. Each run in the design matrix included 7 task-related regressors for 6 tactile stimulation and 1 baseline conditions. The time series for each participant was high-pass-filtered at 1/128 Hz. As the traditional AR (1) + white noise model can fail to whiten the data with short TR, temporal autocorrelations were modelled and estimated from the pooled active voxels by the FAST model, and were used to whiten the data (Corbin et al., 2018). Motion-related artifacts were minimized by incorporating the 6 parameters (3 displacements and 3 rotations) from the rigid-body realignment stage into each model. The contrast estimates for each stimulation condition against baseline condition were evaluated using linear contrasts.

Contrast images from the individual analyses were used for the group analysis, with between-subjects variance modelled as a random factor. The contrast images obtained from the individual analyses represent the normalized task-related increment of the MR signal of each participant. We employed a full factorial design to construct a single design matrix involving 6 conditions. The factors of force and compliance were modelled as within-subject (dependent) levels with unequal variance.

We evaluated the main effect of each factor and their interaction using F tests. The resulting set of voxel values constituted the SPM{F}. The search volume was the whole brain. Brain regions were anatomically defined and labeled in accordance with probabilistic atlases (Shattuck et al., 2008) and an anatomical MR image averaged over all participants.

2.5.2.2. Second analysis (parametric modulation). In the second analysis, we evaluated brain activity positively correlated with the participant's rating of perceived softness. Each run included three task-related regressors: one each for the high-force, low-force condition, and baseline conditions. To reveal the brain areas whose activity co-varied with perceived softness, we performed parametric-modulation analysis (Büchel et al., 1998). We used the participant's trial-by-trial ratings as parametric modulators for each force condition. The regressor for parametric modulators was orthogonalized to that for the task-related regressors. In order to test our prediction that the parietal operculum, the insula, and a part of the occipital cortex are associated with perceived softness regardless of the force magnitude, we evaluated the parametric modulator for each force condition, and then examined their commonalities and differences. The other procedures were identical to the first analysis. We performed one-sample t tests on the contrast estimates obtained from the group analysis. The resulting set of voxel values for each contrast constituted the SPM{t}. We initially conducted the whole-brain analysis and then limited the search volume to the regions that were identified by the localizer experiment (see below).

2.5.3. MVPA

We examined whether the predefined regions of interest (ROIs) contain information on compliance extracted by touch. We constructed new design matrices to obtain parameter estimates and t values for each trial. For each participant, 6 design matrices were produced with each modelling trials in each run. Each regressor in a design matrix modelled BOLD signal during the tactile stimulation in each trial. Thus, each design matrix contained 21 regressors (3 repetitions per run × 6 tactile conditions + 3 repetitions per run for the baseline condition) as well as the 6 motion-related parameters. We generated a map of voxel-wise t-values (SPM{t} map) for each trial of each participant by evaluating the linear contrast of the regressor of each trial against the implicit baseline.

We then performed classification analyses on the voxel-wise t values of each participant (Misaki et al., 2010). A linear support vector machine (MATLAB's SVM) was trained on data obtained from 5 runs. Subsequently, the trained classifier was used to predict compliance of the presented object (soft, medium, or hard) in the remaining run. Accuracy was recorded for the attempted classification of the data. This process was repeated 6 times, using a different run as the test data (leave-one-run-out cross-validation). These cross-validated analyses were performed separately for each ROI.

We combined two approaches to determine whether the performance

of the trained classifier exceed the chance level. First, we used random permutation tests in each region at the single-subject level, and then combines the results at the group level with a bootstrap method (Stelzer et al., 2013). More specifically, we randomly shuffled categories for each t map and then conducted the aforementioned procedure 1000 times for each region of each participant. Then we drew one result (including the original result) from each participant and calculated group-level mean 1000 times. We calculated p value by counting the number of permutations with equal or higher accuracy than the accuracy of the original result and corrected it for multiple comparisons (with Bonferroni correction). Second, we used structures with cerebrospinal blood fluid (CSF) as a control region, because these regions shouldn't contain information related to compliance. The CSF region (21,872 mm^3) was defined based on the high-intensity signal of the mean functional image across the participants. We subtracted the performance of CSF from the classification accuracy in each region and performed non-parametric one-sample test (Wilcoxon signed rank test corrected with Bonferroni correction). We considered that a region contains information about compliance only when both tests showed significant results. We did not use the conventional one-sample *t*-test against the theoretical chance level because it may not provide a valid population inference (Stelzer et al., 2013; Allefeld et al., 2016). Moreover, we can further minimize false positives by examining the accuracy for a control area that does not process any information (Liang et al., 2013; Pilgramm et al., 2016).

We performed the analyses for the following regions that have been previously shown to be involved in tactile object perception (Servos et al., 2001; Bodegard et al., 2003; Kitada et al., 2005, 2006, 2014; Stilla and Sathian, 2008; Sathian et al., 2011; Eck et al., 2013, 2016): the hand area in the postcentral gyrus (21,128 mm^3, z coordinate ranging from 40 to 70), parietal operculum/insula (23,048 mm^3), superior parietal lobule (46,672 mm^3), angular gyrus (33,536 mm^3), supramarginal gyrus (27,776 mm^3), fusiform gyrus (20,496 mm^3), lingual gyrus (25,168 mm^3), middle occipital gyrus (36,800 mm^3), and early visual cortex (corresponding to Brodmann Area 17 and 18, 23,694 mm^3).

The aforementioned ROIs were anatomically defined using Shattuck's probabilistic map (LBPA40; Shattuck et al., 2008) and the probabilistic map in the SPM anatomy toolbox (Eickhoff et al., 2005). Early visual cortex was defined using the anatomical toolbox (Amunts et al., 2000). The parietal operculum/insula were defined by combining the two maps (Eickhoff et al., 2006a, 2006b). Other brain regions were defined using Shattuck's map. The hand area of the postcentral gyrus was defined by limiting Shattuck's map between $z = 40$ and $z = 70$, based on our previous studies (Kitada et al., 2005, 2006; Yang et al., 2017).

We also performed classification analyses to predict the force magnitude corresponding to the presented object. This procedure was identical to the analysis of object compliance, except for the targets of the prediction (high or low force).

2.6. Localizer experiment

The experimental setup was identical to that of the main experiment except that four stimuli were used without manipulating the applied force (Supplementary Fig. 1). A single run consisted of twenty 15-s trials (300 s in total) preceded by 20-s rest and followed by 10-s rest ($300 + 20 + 10 = 330$ s in total, 330 vol). Each condition was repeated 4 times in a single run (4 repetitions × 6 runs = 24 trials for each condition). The order of the 7 conditions in each run was pseudo-randomized. Unlike the main experiment, the onset of the red cross was not jittered in this experiment. The design matrix included 6 runs, with each run containing two task-related regressors: one for tactile stimulation, and the other for the baseline condition. We evaluated softness-related activity using the same parametric modulation analysis employed in the main experiment. We used the result of the localizer experiment to limit the search volume to the anatomically-defined parietal operculum/insula in the univariate analysis (see section 2.5 for the anatomical definition), and extracted parameter estimates of the main experiment at the peak coordinates identified in the localizer experiment. This procedure avoids the invalid statistical inference associated with selection bias (i.e., the double-dipping problem (Kriegeskorte et al., 2009)).

3. Results

3.1. Task performance

Table 1 shows the estimated magnitudes of softness and their response times from the main experiment. Two-way repeated-measures analysis of variance (ANOVA) (3 levels of compliance × 2 levels of force) for rating revealed only a significant main effect of compliance [$F(2, 68) = 1957.4$, $p < 0.001$]. Neither main effect of force nor the interaction effect was significant (p values > 0.8). The post-hoc pairwise comparisons with Bonferroni correction showed that the softness rating was greater for soft stimulus than for other stimuli (p values < 0.001), whereas the rating was higher for the medium stimulus than for hard stimulus (p values < 0.001). The same ANOVA for response time showed only a significant interaction effect [$F(2, 68) = 5.1$, $p < 0.01$]. However, the post-hoc pairwise comparisons with Bonferroni correction showed no significant difference (p values > 0.05).

Similar to the main experiment, the participants were able to estimate softness magnitude of 4 stimuli in the localizer experiment. One-way repeated-measures ANOVA (4 levels of compliance) on rating showed a significant main effect [$F(3, 93) = 969.3$, $p < 0.001$]. Post-hoc pairwise comparisons with Bonferroni correction showed significant differences among all pairs of the stimuli; the higher the compliance was, the higher was the rating (p values < 0.001) (Supplementary Table 1). No significant effect was observed for response time ($p > 0.09$).

3.2. fMRI results

3.2.1. Localizer experiment

The analysis of softness-related brain activity based on the data obtained from the localizer experiment showed graded activation in the left anterior insula, left medial part of the superior frontal gyrus, left posterior insula, and left parietal operculum (Supplementary Table 2 and Supplementary Fig. 2). Based on this result, we limited the search volume to the left parietal operculum and insula, and used peak coordinates to extract parameter estimates in the univariate analysis of the main experiment.

3.2.2. ANOVA (main experiment)

In the analysis of the data obtained from the main experiment, we evaluated F contrasts to depict brain regions involved in the main effects and interaction. Subsequently, we examined brain activity correlated with perceived softness. Finally, we conducted MVPA to examine whether spatial patterns of activity in the ROIs contain information on compliance.

3.2.2.1. Main effects of object compliance. The F contrast for the main

Table 1
Response obtained in the main experiment.

	Soft-low F	Med-low F	Hard-low F	Soft-high F	Med-high F	Hard-high F
Rating	2.86	2.13	1.08	2.87	2.12	1.09
SEM	0.02	0.03	0.03	0.02	0.02	0.03
Response time (ms)	609	604	593	584	618	614
SEM	25	25	22	22	24	22

SEM, standard error of the mean; Soft-low F, high-compliance with the lower force; Med-low F, medium compliance with the lower force; Hard-low F, low compliance with the lower force; Soft-high F, high compliance with the higher force; Med-high F, medium compliance with the higher force; Hard-high F, low compliance with the higher force.

effect of object compliance revealed bilateral regions of significant effect: the postcentral gyrus; precentral gyrus; parietal operculum; insula; superior, middle, and inferior frontal gyri; orbitofrontal cortex; supramarginal gyrus; angular gyrus; superior parietal lobule; precuneus; superior, middle, and inferior temporal gyri; middle occipital gyrus; cingulate gyrus; caudate nucleus; hippocampus; amygdala; and cerebellum (Fig. 2 and Supplementary Table 3). Moreover, we also found unilateral effect in the right lingual gyrus and left parahippocampal gyrus. The representative individual data are provided in the Supplementary Fig. 3.

3.2.2.2. Main effects of force. The F contrast of applied force showed no significant effect.

3.2.2.3. Interactions between object compliance and force. The F contrast of the interaction term showed bilateral regions of significant effect in the superior and middle frontal gyri, cingulate gyrus, superior temporal gyrus, putamen, and caudate nucleus. Moreover, the same test showed significant effect in the left orbitofrontal cortex, left supramarginal gyrus, left angular gyrus, left middle temporal gyrus, left cerebellum, and right posterior insula (Fig. 2 and Supplementary Table 4). The representative individual data are provided in the Supplementary Fig. 4.

3.2.3. Brain regions of which activity is correlated with perceived softness (main experiment)

3.2.3.1. Low-force condition. The whole-brain analysis showed regions of significant activation in the bilateral anterior insula, medial parts of the bilateral superior frontal gyrus, left posterior insula, left parietal operculum, and right cingulate gyrus (Fig. 3A and Supplementary Table 5). The analysis with search volume limited to the parietal operculum and insula showed no additional activation.

3.2.3.2. High-force condition. The whole-brain analysis showed regions of significant activation bilaterally in the anterior insula, parietal operculum, cingulate gyrus, inferior and superior frontal gyri, precentral gyrus, postcentral gyrus, superior parietal lobule, supramarginal gyrus, putamen, and cerebellum. Moreover, the same analysis showed regions of activation in the right hemisphere: the middle frontal gyrus, angular gyrus, caudate nucleus, and lingual gyrus (Fig. 3A and Supplementary Table 6). Further, the analysis with the limited search volume (i.e., the parietal operculum and insula) showed another cluster of significant activation in the left posterior insula and left parietal operculum.

Fig. 3B shows overlap of activation between low-force and high-force conditions. In accordance with the localizer experiment, the overlap was found in the left insula and medial part of the superior frontal gyrus. The overlap in the posterior insula extended to the border between the parietal operculum and insula, whereas the overlap in the superior frontal gyrus extended to the dorsal anterior cingulate gyrus.

3.2.3.3. ROI analysis. We extracted contrast estimates from the peak coordinates defined based on results of the localizer experiment (Fig. 4). Two-way repeated-measures ANOVAs (3 levels of object compliance × 2 levels of applied force) on the contrast estimates (activity relative to baseline) showed significant main effects of object compliance in all regions ($F(2, 68) = 8.03$, $p < 0.01$ for the posterior insula; $F(2, 68) = 6.59$, $p < 0.01$ for the parietal operculum; $F(2, 68) = 17.44$, $p < 0.001$ for the anterior insula; $F(2, 68) = 26.03$, $p < 0.001$ for the superior frontal gyrus). Neither main effect of force nor its interaction was significant (p values > 0.1). Post-hoc pairwise comparisons (with Bonferroni correction) showed that the soft material triggered stronger activity than the hard material in all regions (p values < 0.05). The medium material triggered stronger activity than the hard material in all regions (p values < 0.05), except for the posterior insula ($p = 0.058$). The superior frontal gyrus showed higher activity for the medium material than for the soft material ($p < 0.01$), while no such difference was found in other regions (p-values > 0.5).

3.2.3.4. Difference in softness-related activity between low- and high-force conditions. We then examined the difference in softness-related activity between low- and high-force conditions (i.e., difference of parametric modulators). Within the softness-related regions in the high-force condition, the comparisons between the two force conditions showed stronger softness-related activity in the bilateral putamen and left caudate nucleus in the high-force condition than in the low-force condition (Fig. 5 and Supplementary Table 7). Stronger softness-related activity was not found in the low-force condition than in the high-force condition.

3.2.4. Multi-voxel pattern analysis

We examined which brain regions contain information regarding object compliance by conducting MVPA. Based on the previous studies on material perception (Servos et al., 2001; Bodegard et al., 2003; Kitada et al., 2005, 2014; Stilla and Sathian, 2008; Sathian et al., 2011; Eck

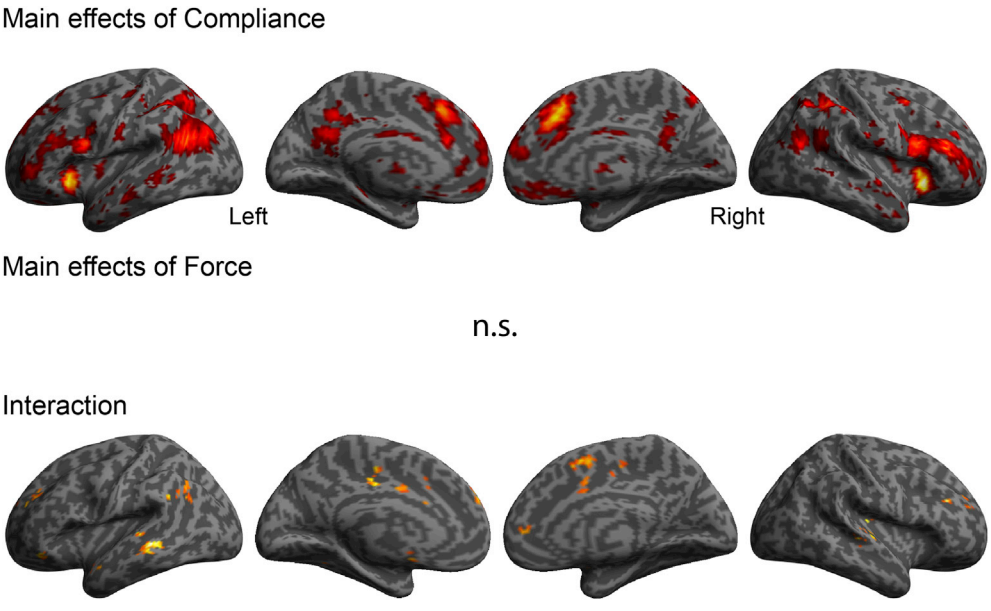

Fig. 2. Main effects and interactions of compliance and applied force.
Main effects and interactions of compliance and applied force were superimposed on a surface-rendered T1-weighted high-resolution magnetic resonance imaging of an individual unrelated to the study. No significant effect was observed for the applied force. The statistical threshold for the spatial extent test was set at $p < 0.05$, family wise error (FWE) corrected for multiple comparisons over the whole brain when the height (cluster-forming) threshold was set at $p < 0.001$ (uncorrected).

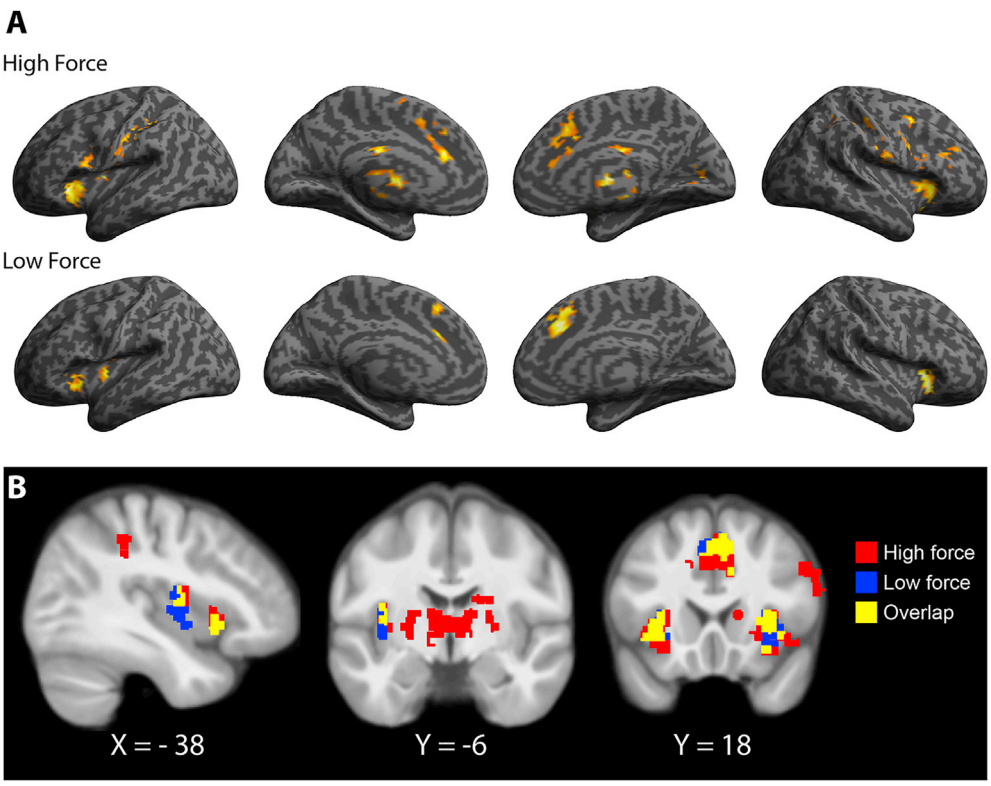

Fig. 3. Brain activity positively correlated with perceived softness.
The statistical threshold for the spatial extent test was set at $p < 0.05$, family-wise error (FWE)-corrected for multiple comparisons when the height threshold was set at $p < 0.001$ (uncorrected). **A.** Brain activation that was positively corrected with perceived softness was superimposed on a surface-rendered T1-weighted high-resolution MRI of an individual unrelated to the study. **B.** Graded activation in the low- and high-force conditions were overlaid on sagittal and coronal sections of the MRIs averaged over the participants.

et al., 2013, 2016), we defined the following anatomical regions as ROIs: the hand area of the postcentral gyrus, insula/parietal operculum, superior parietal lobule, supramarginal gyrus, angular gyrus, early visual cortex (primary and secondary visual cortices), middle occipital gyrus, fusiform gyrus, and lingual gyrus. Permutation tests showed significant results on all regions (p values < 0.01). One-sample Wilcoxon signed rank test on performance accuracy (with Bonferroni correction) showed higher accuracy than control in the postcentral gyrus ($p < 0.001$), insula/parietal operculum ($p < 0.001$), superior parietal lobule ($p < 0.001$), angular gyrus ($p < 0.001$), supramarginal gyrus ($p < 0.001$), and middle occipital gyrus ($p < 0.01$) (Fig. 6). We also conducted the same analysis for the applied force. However, neither permutation nor one-sample Wilcoxon signed-rank test revealed a statistically significant effect (p-values > 0.05).

4. Discussion

In the present study, we examined the brain network of which activity reflects perceived object softness. While a distributed set of brain regions was affected by differences in compliance of stimulus, graded response to perceived softness was limited to the parietal operculum, insula, and superior frontal gyrus. This result was confirmed by the two experiments. Moreover, MVPA showed that not only the parietal operculum and insula, but also the postcentral gyrus, superior parietal lobule, supramarginal gyrus, angular gyrus, and middle occipital gyrus contained information related to object compliance.

4.1. Softness-related activation

To the best of our knowledge, this is the first neuroimaging study to depict the brain activity related to the softness magnitude perceived by touch. Previous neuroimaging studies have shown the involvement of the somatosensory regions in tactile softness perception (Servos et al., 2001; Bodegard et al., 2003). However, because activity during softness perception was compared with that during a control condition that involves no tactile stimulation (e.g., rest), it was unclear to what extent such activity reflects perceived softness. The present study extends these previous findings by demonstrating that a distributed set of the brain regions beyond the primary somatosensory cortex is involved in representing perceived softness magnitude. Furthermore, the most compelling evidence was obtained for the involvement of the parietal operculum (including the secondary somatosensory cortex) and insula in such representation; these regions showed graded response to perceived softness in the two experiments performed in this study. This result indicates that this region constitutes an important node of the brain network involved in processing object compliance for tactile softness perception. This result is consistent with a previous finding that ablation of the secondary somatosensory cortex in monkeys causes impairment of haptic discrimination of softness and roughness (Murray and Mishkin, 1984).

Neuroimaging studies have also shown that activity in these regions is related to perceived roughness (Kitada et al., 2005; Eck et al., 2016) and temperature (Craig et al., 2000). A patient with a tumor compressing the parietal operculum and insula demonstrated a relatively poor ability to discriminate the roughness of abrasives (Greenspan and Winfield, 1992). Thus, the present finding, in conjunction with the previous findings, supports the hypothesis that the parietal operculum and insula play a critical role in extracting intensity information of material properties (Roland et al., 1998; Kitada, 2016; Sathian, 2016). Thus, this is consistent with the idea that the two major categories of tangible object properties—macro-geometric and material properties—are processed in overlapping, but distinct, brain networks (Kitada, 2016; Sathian, 2016).

As object compliance is negatively correlated with the applied force (Fig. 1B), softness-related activity can be explained by the difference in force imposed on the finger. In order to examine this further, we examined the effect of force on the pattern of graded activity. Although no brain region showed a significant main effect of force, all the participants could easily perceive the difference in the applied force. More importantly, we observed significant interactions between the applied force and perceived softness. Thus, the difference in the applied force should be sufficiently large to examine its effect on softness-related activity. Nevertheless, the regions in the parietal operculum and insula showed highly similar patterns of graded activity. This result indicates that these

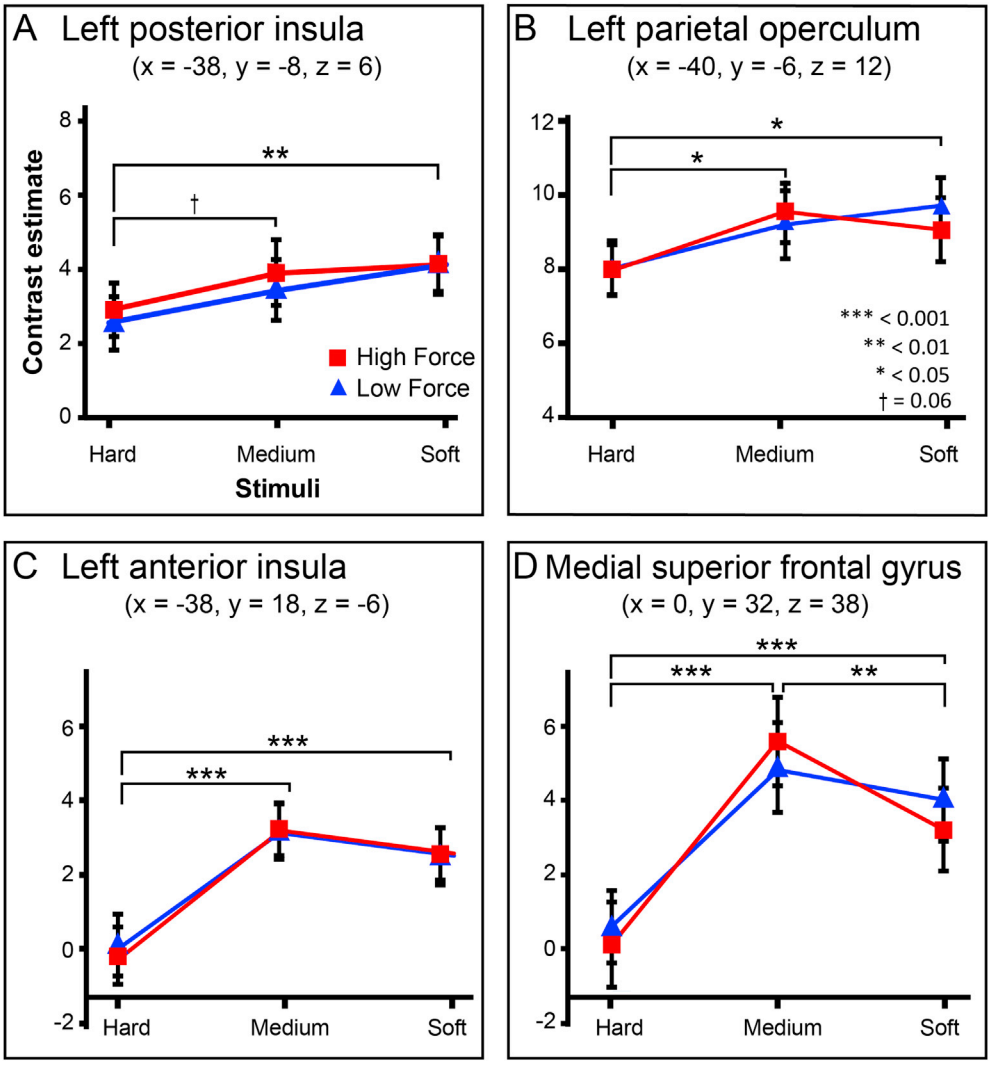

Fig. 4. ROI analysis.
Contrast estimates in the first analysis (analysis of variance) of the main experiment were extracted from the regions of interest (ROI) defined using the results of the localizer experiment. Two-way repeated-measures ANOVA (3 levels of compliance × 2 levels of applied force) on contrast estimates showed significant main effects of compliance (p values < 0.01) without interaction effect (p values > 0.1). Post hoc pairwise comparisons with Bonferroni correction revealed significantly greater activity in all the regions in the soft condition than in the hard condition (p values < 0.05).

regions are not simply related to the applied force, but involved in representing compliance of the object. Indeed, the participants rated the perceived softness similarly regardless of the force imposed on the finger (Table 1), indicating perceptual constancy against applied force. This is analogous to perceptual constancy of roughness against speed; physical roughness and compliance are enduring features of an object, and hence, it is important that the corresponding percepts remains relatively invariant, regardless of how the finger contacts the surface (Kitada et al., 2012; Lederman et al., 1983; Meftah el et al., 2000).

It is proposed that the insula represents all aspects of the physiological condition of the body. This system constitutes a representation of "the material me," and might provide a foundation for subjective feelings, emotion, and self-awareness (Craig, 2002). For instance, the insula is also sensitive to pain (Coghill et al., 1999), itch (Mochizuki et al., 2007), and brush stimulus causing pleasantness (Olausson et al., 2002). Material properties such as roughness can be highly associated with the affective aspects of touch (Kitada et al., 2012). In the present study, participants appeared to perceive the softer stimulus as more pleasant (agreed on by all the experimenters). Thus, it is possible that the insula represents the information on affective feelings associated with the magnitude of the perceived softness. In other words, the insula may be a region that connects the discriminative (e.g., softness) and affective aspects (e.g., pleasantness) of touch.

We also observed graded response in the superior frontal gyrus, including the dorsal anterior cingulate cortex (ACC). The anterior insula and ACC are often activated together and hence regarded as complementary limbic regions (Craig, 2009). Thus, it is possible that the ACC works with the insula in a network to represent softness and its associated affective feelings. However, the ROI analysis showed that this region was most sensitive to the medium stimulus, which is difficult to be explained by this speculation. The alternative interpretation is that this region is related to task difficulty. For instance, when the participants touch the softest stimulus, they tend to consider the softest and medium stimuli before identifying the correct one. On the other hand, when they touch the medium stimulus, they must consider all three stimuli to identify the correct one. This speculation is consistent with the previous finding that this region is involved in choice difficulty, as in selection among a set of equally permissible responses (Botvinick, 2007; Shenhav et al., 2014).

Softness-related activity in the putamen was greater in the high-force than in the low-force condition. One explanation is that the putamen is also involved in processing softness. The putamen is related to categorization of tactually perceived speeds (Romo et al., 1995; Merchant et al., 1997). Since higher applied force causes more deformation of the stimulus, the relationship between an applied force and the resulting deformation can become salient. Thus, such salience may be associated with greater softness-related activity in the putamen. Alternatively, softer stimulus in the present study was perceived more pleasant than harder ones, and larger deformation due to the higher applied force could have induced more pleasant feelings. The activity of the putamen was detected in and adjacent to the ventral striatum, regions activated by reward

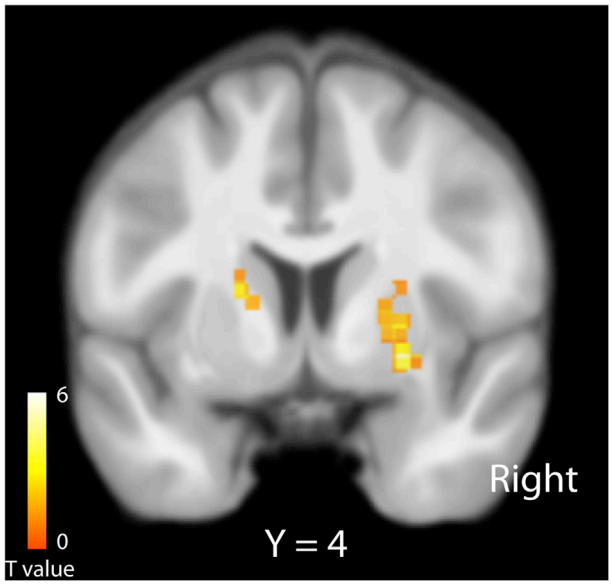

Fig. 5. Difference in softness-related activity between the two applied forces. Greater softness-related activity in the high-force than low-force condition was shown on a coronal section of the T1-weighted high-resolution MRIs averaged over the participants. No greater softness-related activity in the low-force condition than high-force condition was found. The statistical threshold for the spatial extent test was set at $p < 0.05$, family wise error (FWE) corrected for multiple comparisons over the whole brain when the height threshold was set at $p < 0.001$ (uncorrected).

(Sacchet and Knutson, 2013; Sumiya et al., 2017). It is possible that the affective aspect of softness perception caused different compliance-related activation in the putamen.

4.2. MVPA

We found that voxels in the postcentral gyrus, parietal operculum/insula, posterior parietal lobule, and middle occipital gyrus could decode the stimuli more accurately than the chance level. This result indicates that these regions contain information related to object compliance. Tactile perception of softness is based on the spatio-temporal variation of pressure on the skin (Srinivasan and LaMotte, 1996). Thus, perception of softness and coarse roughness can rely on signals from the slowly adapting type I (SA-I) fibers in the periphery (Srinivasan and LaMotte, 1996; Weber et al., 2013). The primary somatosensory cortex in the postcentral gyrus of non-human primates contains neurons that encode roughness (Bourgeon et al., 2016; Sinclair and Burton et al., 1991) and applied force (Sinclair and Burton et al., 1991). Thus, one interpretation is that the actual calculation of the perceived softness is performed in the postcentral gyrus, and such information is sent to the parietal operculum and insula. If this is the case, this region should also contain information on the applied force that is required to calculate compliance (i.e., deformation relative to an imposed force). However, voxels in this region did not decode the two levels of force more accurately than the chance level. Therefore, future studies are necessary to examine how signals associated with the applied force and magnitude of deformation are extracted, and used to represent softness in these brain regions.

The superior parietal lobule and supramarginal gyrus also contained information on object compliance. One interpretation of this result is that these regions are also involved in the perception of hardness. In other words, objects must be sufficiently hard for their shapes to be perceived. For instance, the soft stimulus used in this study could be easily deformed, and hence, it is difficult to perceive its actual shape. Thus, the perception of hard objects may be associated with their shape perception. This speculation is consistent with the findings that these regions are more involved in processing macro-spatial properties than material properties (Kitada et al., 2006; Roland et al., 1998; Stilla and Sathian, 2008).

Finally, the higher performance accuracy than chance level and the control region in the middle occipital gyrus is in accordance with the result of the mass univariate analysis (main effect of compliance). This is also consistent with previous findings that a part of the occipital cortex may be more strongly active during the tactile perception of textures than of macro-spatial object properties such as shape (Stilla and Sathian, 2008), orientation (Kitada et al., 2006), and relative position (Sathian et al., 2011). Especially, the middle occipital gyrus includes a region that shows greater activity in response to textures than locations of dots, regardless of the sensory modality (Sathian et al., 2011). One possible

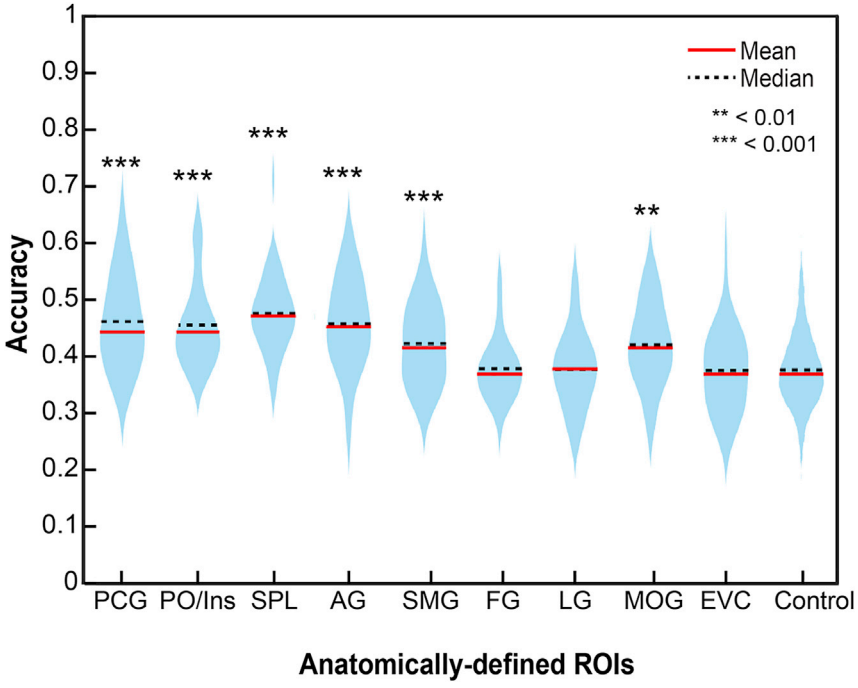

Fig. 6. Multi-voxel pattern analysis on object compliance. Distributions of accuracy based on MVPA. Asterisks indicate the result of Wilcoxon signed rank tests on accuracy relative to that of the CSF region (Control) (with Bonferroni correction). PCG, postcentral gyrus; PO/Ins, parietal operculum/insula; SPL, superior parietal lobule; SMG, supramarginal gyrus, AG, angular gyrus; FG, fusiform gyrus; LG, lingual gyrus; MOG, middle occipital gyrus; EVC, early visual cortex (anatomically defined primary and secondary visual cortices).

explanation of this result is that activation of the occipital cortex during tactile texture perception is associated with the visual-mediation strategy (Lederman et al., 1990; Sathian et al., 1997). More specifically, it is possible to retrieve visual information that was previously associated with the tactile sensation of an object (Kitada et al., 2014). Retrieval of this information may lead to the observed effect of object compliance on the activity of this region. This speculation is also supported by our finding that the hippocampus and precuneus also showed a main effect of compliance because these regions are involved in the visuo-tactile association of textures (Kitada et al., 2014). Alternatively, this region may play other roles in tactile processing; however, further investigation is required to confirm whether this region is indeed necessary for tactile texture processing (e.g., brain stimulation studies).

4.3. Interpretational issues

In the present study, we jittered the onset of response relative to tactile stimulation, and only tactile stimulation was modelled in the analysis. Moreover, the order of responses was counterbalanced across the participants. Thus, softness-related activity in the parietal operculum and insula, which was revealed by the univariate analysis, cannot be explained by finger movements for a specific response. Moreover, we focused on the left hemisphere, which is contralateral to the hand being stimulated. Thus, although the multivariate analysis may be more sensitive to signals associated with the responses than univariate analysis, this is likely to cause negligible effect, if any, on the patterns of performance accuracy in the left hemisphere.

5. Conclusions

To our best knowledge, the present study is the first neuroimaging study that revealed brain networks associated with softness magnitudes perceived by touch. We found that a distributed set of brain regions is related to the perception of softness. Of these, the parietal operculum and insula showed graded response to perceived softness, whereas the postcentral gyrus, superior parietal lobule, supramarginal gyrus, and the middle occipital gyrus contained some information related to perceived softness. This result indicates that the parietal operculum and insula constitute an important node of the brain network for tactile softness perception, which also involves the primary somatosensory cortex, posterior parietal lobule, and occipital cortex. Therefore, the parietal operculum and insula may be involved in representation of haptically-perceived material properties, regardless of the perceptual dimensions.

Declaration of interest

The authors declare no conflict of interest.

Acknowledgments

The multiband EPI sequence was provided by the Center for Magnetic Resonance Research, University of Minnesota. We thank Mr. Yoshikuni Ito and Mr. Rajaei Nader for their technical assistance.

Appendix A. Supplementary data

Supplementary data to this article can be found online at https://doi.org/10.1016/j.neuroimage.2019.04.044.

Funding

This work was supported by MEXT/JSPS KAKENHI (grant number: 16H01680, 25135734), and an NAP startup grant from the Nanyang Technological University to R.K., MEXT/JSPS KAKENHI grants to M.S. (grant number: 25135713, 15H05922), H.K. (grant number: 15H05923), and N.S. (grant numbers: 26244031 and 15H01846). This research is partially supported by Japan Agency for Medical Research and Development (grant number JP18dm0107152 and JP18dm0307001) to N.S..

Authors contributions

Author contributions: R.K., M.S., H.K., and N.S. designed the study; R.K., R.D., J.K., T.T., and E.N. performed the experiments; H.K. and T.K. contributed reagents and unpublished analytic tools; R.K. analyzed data and wrote the paper.

References

Allefeld, C., Görgen, K., Haynes, J.D., 2016. Valid population inference for information-based imaging: from the second-level t-test to prevalence inference. Neuroimage 141, 378–392. https://doi.org/10.1016/j.neuroimage.2016.07.040.

Amunts, K., Malikovic, A., Mohlberg, H., Schormann, T., Zilles, K., 2000. Brodmann's areas 17 and 18 brought into stereotaxic space-where and how variable? Neuroimage 11, 66–84. https://doi.org/10.1006/nimg.1999.0516.

Ashburner, J., 2007. A fast diffeomorphic image registration algorithm. Neuroimage 38, 95–113. https://doi.org/10.1016/j.neuroimage.2007.07.007.

Bodegard, A., Geyer, S., Herath, P., Grefkes, C., Zilles, K., Roland, P.E., 2003. Somatosensory areas engaged during discrimination of steady pressure, spring strength, and kinesthesia. Hum. Brain Mapp. 20, 103–115. https://doi.org/10.1002/hbm.10125.

Botvinick, M.M., 2007. Conflict monitoring and decision making: reconciling two perspectives on anterior cingulate function. Cognit. Affect Behav. Neurosci. 7, 356–366. https://doi.org/10.3758/CABN.7.4.356.

Bourgeon, S., Depeault, A., Meftah el, M., Chapman, C.E., 2016. Tactile texture signals in primate primary somatosensory cortex and their relation to subjective roughness intensity. J. Neurophysiol. 115, 1767–1785. https://doi.org/10.1152/jn.00303.2015.

Büchel, C., Holmes, A.P., Rees, G., Friston, K.J., 1998. Characterizing stimulus-response functions using nonlinear regressors in parametric fMRI experiments. Neuroimage 8, 140–148. https://doi.org/10.1006/nimg.1998.0351.

Coghill, R.C., Sang, C.N., Maisog, J.M., Iadarola, M.J., 1999. Pain intensity processing within the human brain: a bilateral, distributed mechanism. J. Neurophysiol. 82, 1934–1943. https://doi.org/10.1152/jn.1999.82.4.1934.

Corbin, N., Todd, N., Friston, K.J., Callaghan, M.F., 2018. Accurate modeling of temporal correlations in rapidly sampled fMRI time series. Hum. Brain Mapp. 39, 3884–3897. https://doi.org/10.1002/hbm.24218.

Craig, A.D., 2002. How do you feel? Interoception: the sense of the physiological condition of the body. Nat. Rev. Neurosci. 3, 655–666. https://doi.org/10.1038/nrn894.

Craig, A.D., 2009. How do you feel–now? The anterior insula and human awareness. Nat. Rev. Neurosci. 10, 59–70. https://doi.org/10.1038/nrn2555.

Craig, A.D., Chen, K., Bandy, D., Reiman, E.M., 2000. Thermosensory activation of insular cortex. Nat. Neurosci. 3, 184–190. https://doi.org/10.1038/72131.

Eck, J., Kaas, A.L., Goebel, R., 2013. Crossmodal interactions of haptic and visual texture information in early sensory cortex. Neuroimage 75, 123–135. https://doi.org/10.1016/j.neuroimage.2013.02.075.

Eck, J., Kaas, A.L., Mulders, J.L., Hausfeld, L., Kourtzi, Z., Goebel, R., 2016. The effect of task instruction on haptic texture processing: the neural underpinning of roughness and spatial density perception. Cerebr. Cortex 26, 384–401. https://doi.org/10.1093/cercor/bhu294.

Eickhoff, S.B., Amunts, K., Mohlberg, H., Zilles, K., 2006a. The human parietal operculum. II. Stereotaxic maps and correlation with functional imaging results. Cerebr. Cortex 16, 268–279. https://doi.org/10.1093/cercor/bhi106.

Eickhoff, S.B., Schleicher, A., Zilles, K., Amunts, K., 2006b. The human parietal operculum. I. Cytoarchitectonic mapping of subdivisions. Cerebr. Cortex 16, 254–267. https://doi.org/10.1093/cercor/bhi105.

Eickhoff, S.B., Stephan, K.E., Mohlberg, H., Grefkes, C., Fink, G.R., Amunts, K., Zilles, K., 2005. A new SPM toolbox for combining probabilistic cytoarchitectonic maps and functional imaging data. Neuroimage 25, 1325–1335. https://doi.org/10.1016/j.neuroimage.2004.12.034.

Feinberg, D.A., Moeller, S., Smith, S.M., Auerbach, E., Ramanna, S., Gunther, M., Glasser, M.F., Miller, K.L., Ugurbil, K., Yacoub, E., 2010. Multiplexed echo planar imaging for sub-second whole brain FMRI and fast diffusion imaging. PLoS One 5, e15710. https://doi.org/10.1371/journal.pone.0015710.

Friston, K.J., Ashburner, J., Kiebel, S.J., Nichols, T.E., Penny, W.D., 2007. Statistical Parametric Mapping: the Analysis of Functional Brain Images. Academic Press, London.

Flandin, G., Friston, K.J., 2019. Analysis of family-wise error rates in statistical parametric mapping using random field theory. Hum. Brain Mapp. 40, 2052–2054. https://doi.org/10.1002/hbm.23839.

Greenspan, J.D., Winfield, J.A., 1992. Reversible pain and tactile deficits associated with a cerebral tumor compressing the posterior insula and parietal operculum. Pain 50, 29–39. https://doi.org/10.1016/0304-3959(92)90109-O.

Hollins, M., Bensmaïa, S., Karlof, K., Young, F., 2000. Individual differences in perceptual space for tactile textures: evidence from multidimensional scaling. Percept. Psychophys. 62, 1534–1544. https://doi.org/10.3758/BF03212154.

Hollins, M., Faldowski, R., Rao, S., Young, F., 1993. Perceptual dimensions of tactile surface texture: a multidimensional scaling analysis. Percept. Psychophys. 54, 697–705. https://doi.org/10.3758/BF03211795.

Jones, L.A., Lederman, S.J., 2006. Human Hand Function. Oxford University Press, New York. https://doi.org/10.1093/acprof:oso/9780195173154.001.0001.
Kitada, R., 2016. The brain network for haptic object recognition. In: Kajimoto, H., Saga, S., Konyo, M. (Eds.), Pervasive Haptics. Springer Press, Tokyo, pp. 22–37.
Kitada, R., Hashimoto, T., Kochiyama, T., Kito, T., Okada, T., Matsumura, M., Lederman, S.J., Sadato, N., 2005. Tactile estimation of the roughness of gratings yields a graded response in the human brain: an fMRI study. Neuroimage 25, 90–100. https://doi.org/10.1016/j.neuroimage.2004.11.026.
Kitada, R., Kito, T., Saito, D.N., Kochiyama, T., Matsumura, M., Sadato, N., Lederman, S.J., 2006. Multisensory activation of the intraparietal area when classifying grating orientation: a functional magnetic resonance imaging study. J. Neurosci. 26, 7491–7501. https://doi.org/10.1523/JNEUROSCI.0822-06.2006.
Kitada, R., Sadato, N., Lederman, S.J., 2012. Tactile perception of nonpainful unpleasantness in relation to perceived roughness: effects of inter-element spacing and speed of relative motion of rigid 2-D raised-dot patterns at two body loci. Perception 41, 204–220. https://doi.org/10.1068/p7168.
Kitada, R., Sasaki, A.T., Okamoto, Y., Kochiyama, T., Sadato, N., 2014. Role of the precuneus in the detection of incongruency between tactile and visual texture information: a functional MRI study. Neuropsychologia 64, 252–262. https://doi.org/10.1016/j.neuropsychologia.2014.09.028.
Kriegeskorte, N., Simmons, W.K., Bellgowan, P.S., Baker, C.I., 2009. Circular analysis in systems neuroscience: the dangers of double dipping. Nat. Neurosci. 12, 535–540. https://doi.org/10.1038/nn.2303.
Lederman, S.J., 1983. Tactual roughness perception: spatial and temporal determinants. Can. J. Psychol. 37, 498–511. https://doi.org/10.1037/h0080750.
Lederman, S.J., Klatzky, R.L., 1997. Relative availability of surface and object properties during early haptic processing. J. Exp. Psychol. Hum. Percept. Perform. 23, 1680–1707. https://doi.org/10.1037/0096-1523.23.6.1680.
Lederman, S.J., Klatzky, R.L., Chataway, C., Summers, C.D., 1990. Visual mediation and the haptic recognition of two-dimensional pictures of common objects. Percept. Psychophysiology 47, 54–64. https://doi.org/10.3758/BF03208164.
Lederman, S.J., Taylor, M.M., 1972. Fingertip force, surface geometry and the perception of roughness by active touch. Percept. Psychophys. 12, 401–408. https://doi.org/10.3758/BF03205850.
Liang, M., Mouraux, A., Hu, L., Iannetti, G.D., 2013. Primary sensory cortices contain distinguishable spatial patterns of activity for each sense. Nat. Commun. 4, 1979. https://doi.org/10.1038/ncomms2979.
Meftah el, M., Belingard, L., Chapman, C.E., 2000. Relative effects of the spatial and temporal characteristics of scanned surfaces on human perception of tactile roughness using passive touch. Exp. Brain Res. 132, 351–361. https://doi.org/10.1007/s002210000348.
Merchant, H., Zainos, A., Hernandez, A., Salinas, E., Romo, R., 1997. Functional properties of primate putamen neurons during the categorization of tactile stimuli. J. Neurophysiol. 77, 1132–1154. https://doi.org/10.1152/jn.1997.77.3.1132.
Misaki, M., Kim, Y., Bandettini, P.A., Kriegeskorte, N., 2010. Comparison of multivariate classifiers and response normalizations for pattern-information fMRI. Neuroimage 53, 103–118. https://doi.org/10.1016/j.neuroimage.2010.05.051.
Mochizuki, H., Sadato, N., Saito, D.N., Toyoda, H., Tashiro, M., Okamura, N., Yanai, K., 2007. Neural correlates of perceptual difference between itching and pain: a human fMRI study. Neuroimage 36, 706–717. https://doi.org/10.1016/j.neuroimage.2007.04.003.
Murray, E.A., Mishkin, M., 1984. Relative contributions of SII and area 5 to tactile discrimination in monkeys. Behav. Brain Res. 11, 67–83. https://doi.org/10.1016/0166-4328(84)90009-3.
Olausson, H., Lamarre, Y., Backlund, H., Morin, C., Wallin, B.G., Starck, G., Ekholm, S., Strigo, I., Worsley, K., Vallbo, A.B., Bushnell, M.C., 2002. Unmyelinated tactile afferents signal touch and project to insular cortex. Nat. Neurosci. 5, 900–904. https://doi.org/10.1038/nn896.
Oldfield, R.C., 1971. The assessment and analysis of handedness: the Edinburgh inventory. Neuropsychologia 9, 97–113. https://doi.org/10.1016/0028-3932(71)90067-4.
Oosterhof, N.N., Connolly, A.C., Haxby, J.V., 2016. CoSMoMVPA: multi-modal multivariate pattern analysis of neuroimaging data in Matlab/GNU Octave. Front. Neuroinf. 10, 27. https://doi.org/10.3389/fninf.2016.00027.
Pilgramm, S., de Haas, B., Helm, F., Zentgraf, K., Stark, R., Munzert, J., Krüger, B., 2016. Motor imagery of hand actions: decoding the content of motor imagery from brain activity in frontal and parietal motor areas. Hum. Brain Mapp. 37, 81–93. https://doi.org/10.1002/hbm.23015.
Rajaei, N., Aoki, N., Takahashi, H.K., Miyaoka, T., Kochiyama, T., Ohka, M., Sadato, N., Kitada, R., 2018. Brain networks underlying conscious tactile perception of textures as revealed using the velvet hand illusion. Hum. Brain Mapp. 39, 4787–4801. https://doi.org/10.1002/hbm.24323.
Roland, P.E., O'Sullivan, B., Kawashima, R., 1998. Shape and roughness activate different somatosensory areas in the human brain. Proc. Natl. Acad. Sci. U. S. A 95, 3295–3300. https://doi.org/10.1073/pnas.95.6.3295.
Romo, R., Merchant, H., Ruiz, S., Crespo, P., Zainos, A., 1995. Neuronal-activity of primate putamen during categorical perception of somatesthetic stimuli. Neuroreport 6, 1013–1017.
Sacchet, M.D., Knutson, B., 2013. Spatial smoothing systematically biases the localization of reward-related brain activity. Neuroimage 66, 270–277. https://doi.org/10.1016/j.neuroimage.2012.10.056.
Sathian, K., 2016. Analysis of haptic information in the cerebral cortex. J. Neurophysiol. 116, 1795–1806. https://doi.org/10.1152/jn.00546.2015.
Sathian, K., Lacey, S., Stilla, R., Gibson, G.O., Deshpande, G., Hu, X., Laconte, S., Glielmi, C., 2011. Dual pathways for haptic and visual perception of spatial and texture information. Neuroimage 57, 462–475. https://doi.org/10.1016/j.neuroimage.2011.05.001.
Sathian, K., Zangaladze, A., Hoffman, J.M., Grafton, S.T., 1997. Feeling with the mind's eye. Neuroreport 8, 3877–3881.
Servos, P., Lederman, S., Wilson, D., Gati, J., 2001. fMRI-derived cortical maps for haptic shape, texture, and hardness. Cogn. Brain Res. 12, 307–313. https://doi.org/10.1016/S0926-6410(01)00041-6.
Shattuck, D.W., Mirza, M., Adisetiyo, V., Hojatkashani, C., Salamon, G., Narr, K.L., Poldrack, R.A., Bilder, R.M., Toga, A.W., 2008. Construction of a 3D probabilistic atlas of human cortical structures. Neuroimage 39, 1064–1080. https://doi.org/10.1016/j.neuroimage.2007.09.031.
Shenhav, A., Straccia, M.A., Cohen, J.D., Botvinick, M.M., 2014. Anterior cingulate engagement in a foraging context reflects choice difficulty, not foraging value. Nat. Neurosci. 17, 1249–1254. https://doi.org/10.1038/nn.3771.
Sinclair, R.J., Burton, H., 1991. Neuronal activity in the primary somatosensory cortex in monkeys (Macaca mulatta) during active touch of textured surface gratings: responses to groove width, applied force, and velocity of motion. J. Neurophysiol. 66, 153–169. https://doi.org/10.1152/jn.1991.66.1.153.
Srinivasan, M.A., LaMotte, R.H., 1995. Tactual discrimination of softness. J. Neurophysiol. 73, 88–101. https://doi.org/10.1152/jn.1995.73.1.88.
Srinivasan, M.A., LaMotte, R.H., 1996. Tactual discrimination of softness: abilities and mechanisms. In: Franzén, O., J.R, Terenius, L. (Eds.), Somesthesis and the Neurobiology of the Somatosensory Cortex. Advances in Life Sciences. Birkhäuser, Basel.
Stelzer, J., Chen, Y., Turner, R., 2013. Statistical inference and multiple testing correction in classification-based multi-voxel pattern analysis (MVPA): random permutations and cluster size control. Neuroimage 65, 69–82.
Stilla, R., Sathian, K., 2008. Selective visuo-haptic processing of shape and texture. Hum. Brain Mapp. 29, 1123–1138. https://doi.org/10.1002/hbm.20456.
Sumiya, M., Koike, T., Okazaki, S., Kitada, R., Sadato, N., 2017. Brain networks of social action-outcome contingency: the role of the ventral striatum in integrating signals from the sensory cortex and medial prefrontal cortex. Neurosci. Res. 123, 43–54. https://doi.org/10.1016/j.neures.2017.04.015.
Weber, A.I., Saal, H.P., Lieber, J.D., Cheng, J.W., Manfredi, L.R., Dammann 3rd, J.F., Bensmaia, S.J., 2013. Spatial and temporal codes mediate the tactile perception of natural textures. Proc. Natl. Acad. Sci. U. S. A 110, 17107–17112. https://doi.org/10.1073/pnas.1305509110.
Yang, J., Kitada, R., Kochiyama, T., Yu, Y., Makita, K., Araki, Y., Wu, J., Sadato, N., 2017. Brain networks involved in tactile speed classification of moving dot patterns: the effects of speed and dot periodicity. Sci. Rep. 7, 40931.
Zeki, S., 1998. Parallel processing, asynchronous perception, and a distributed system of consciousness in vision. Neuroscientist 4, 365–372. https://doi.org/10.1177/107385849800400518.